

8.7 Figures

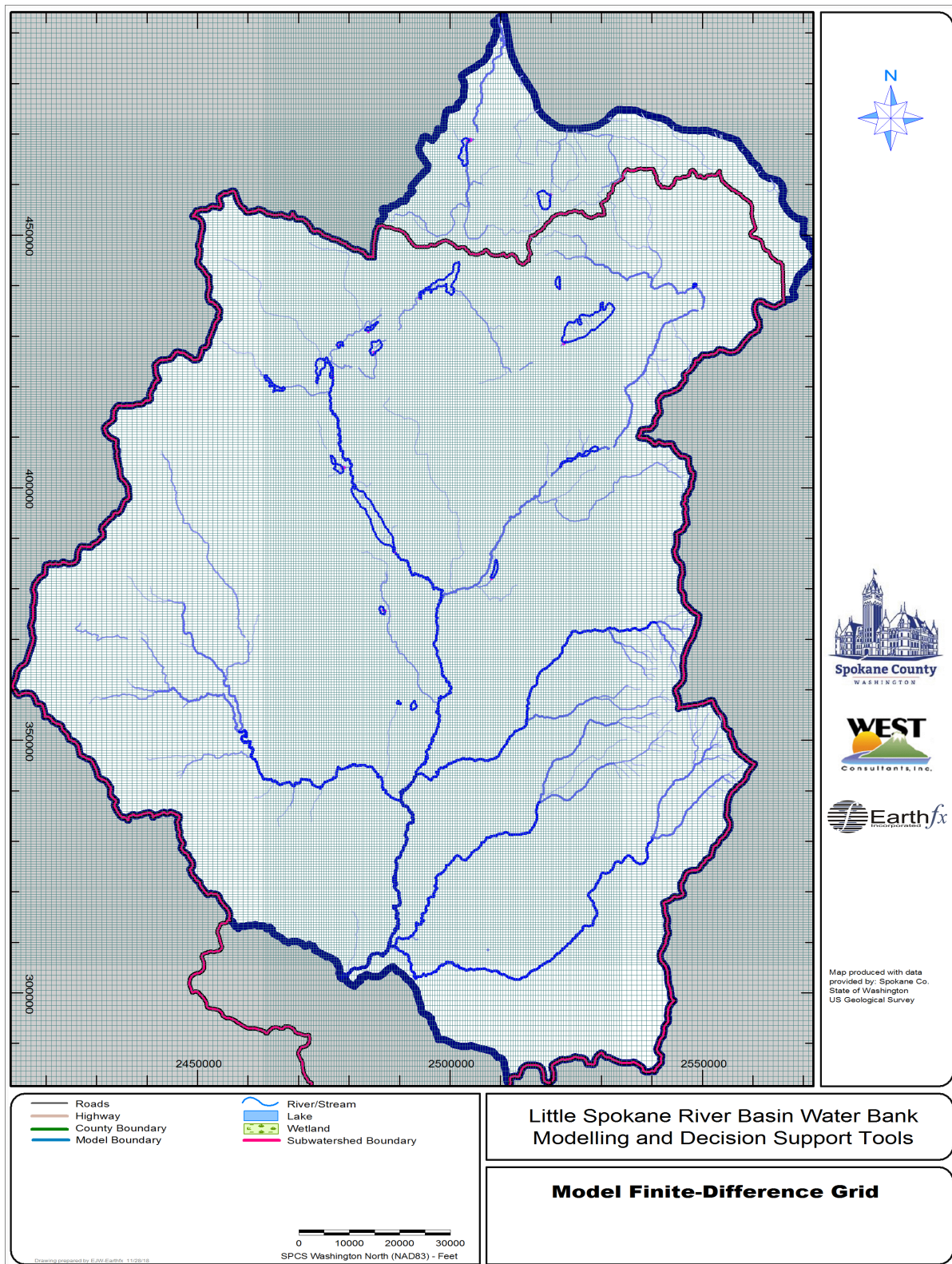


Figure 8.4: Finite-difference grid for the LSR Model.

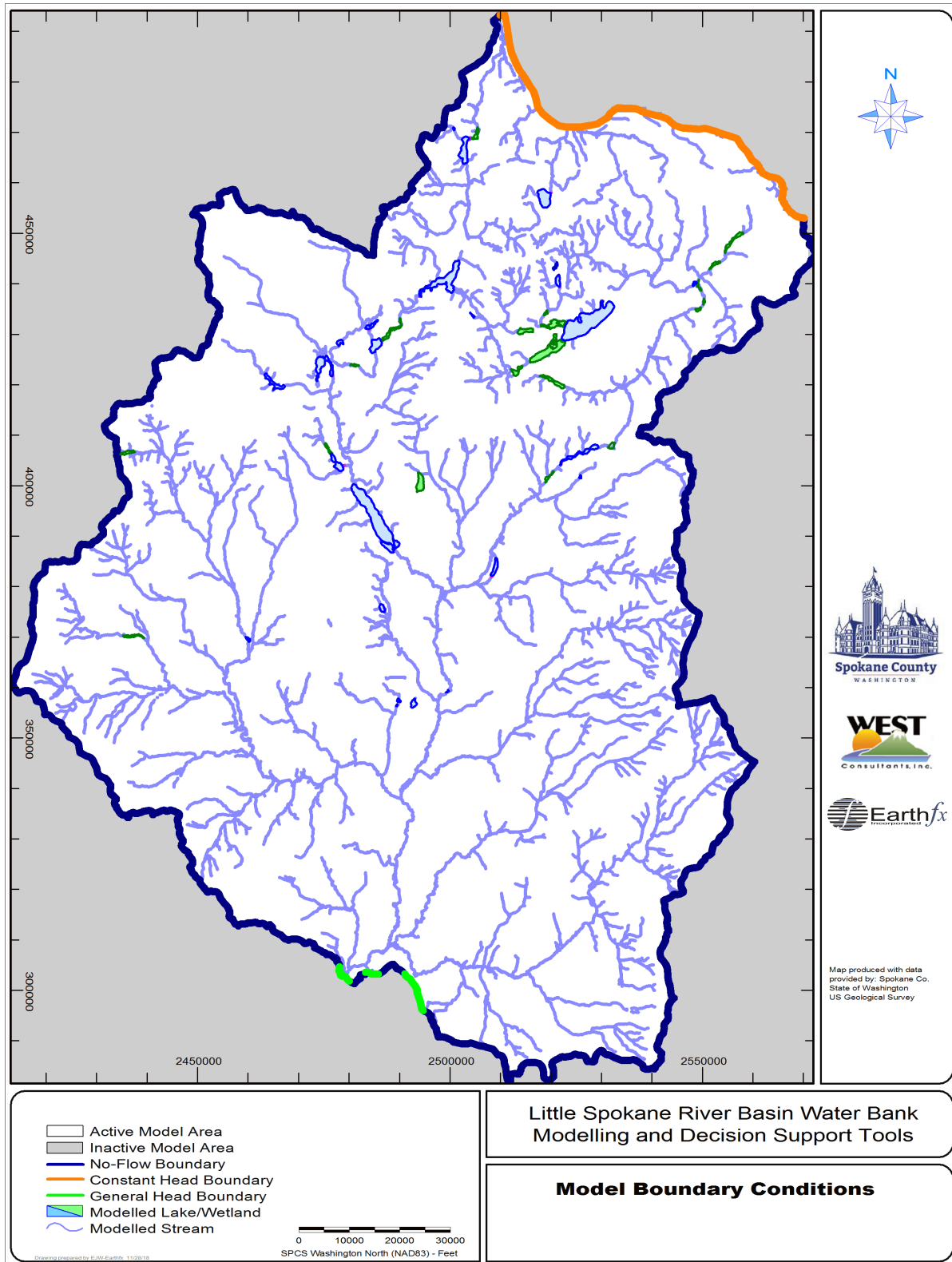


Figure 8.5: Boundary conditions for the numerical groundwater flow submodel.

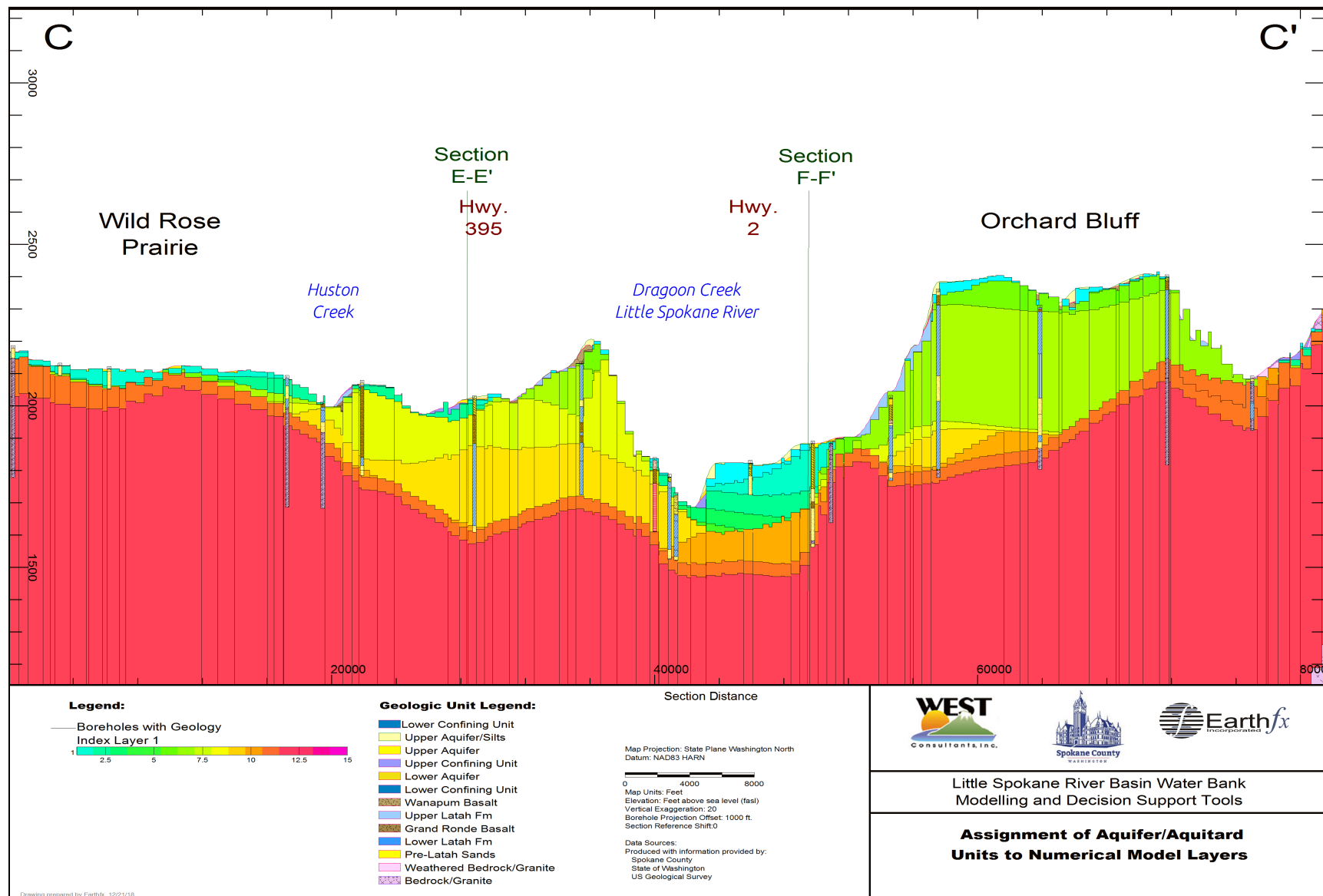


Figure 8.6: Section C-C' showing assignment of aquifer units to numerical model layers.

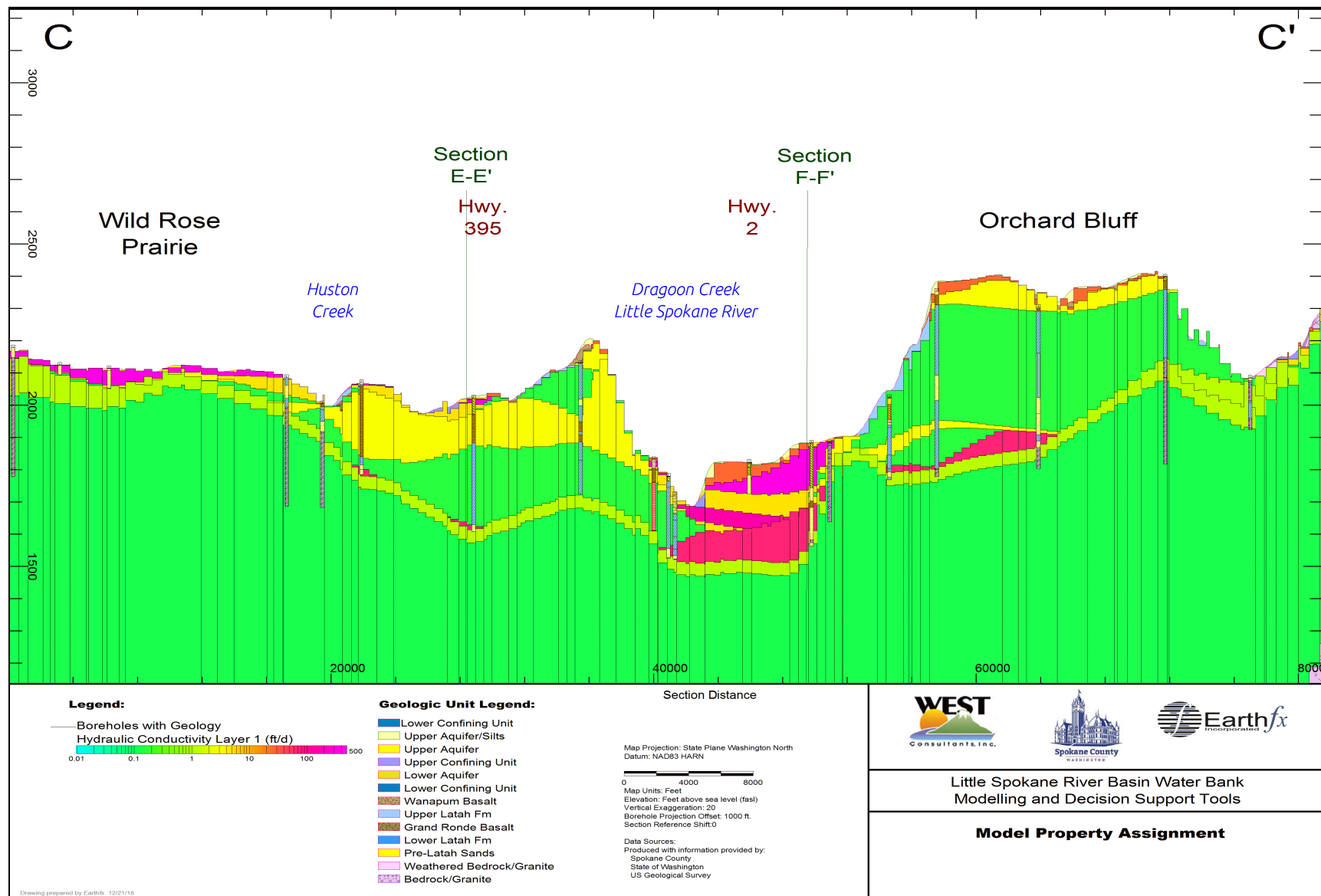


Figure 8.7: Section C-C' showing assignment of hydraulic conductivity to numerical model layers.

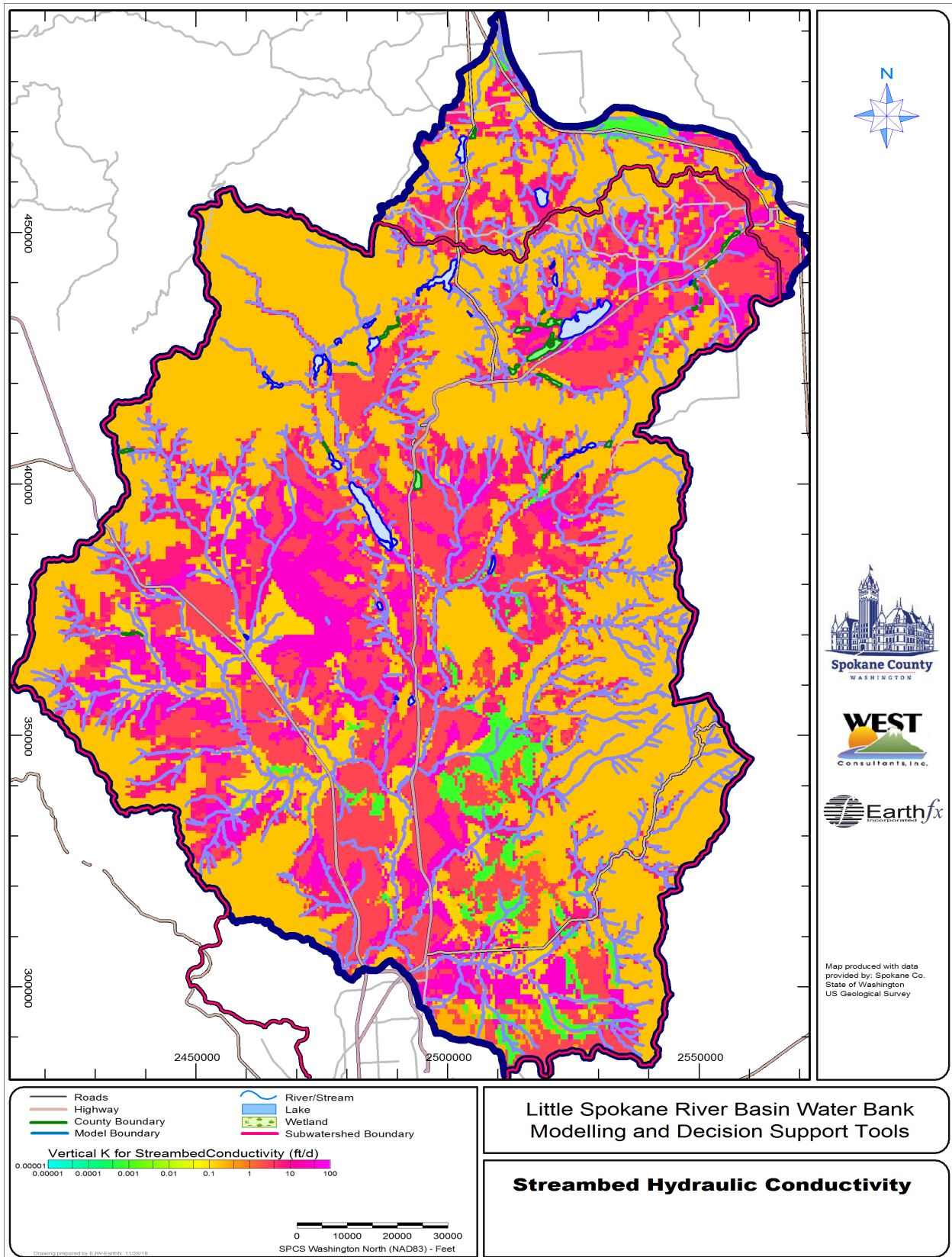


Figure 8.8: Streambed hydraulic conductivity.

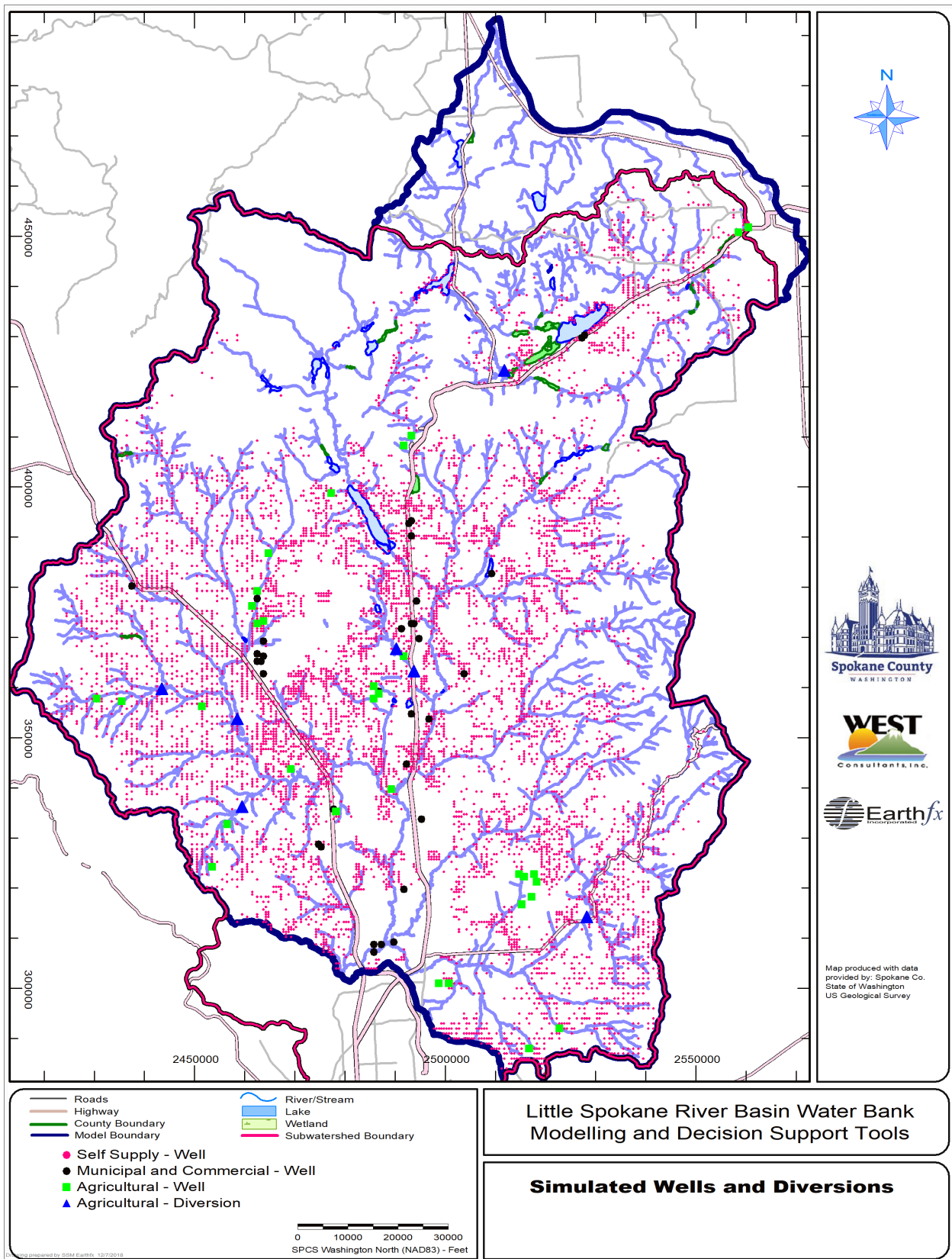


Figure 8.9: Locations of groundwater withdrawals and surface water diversions in the model.

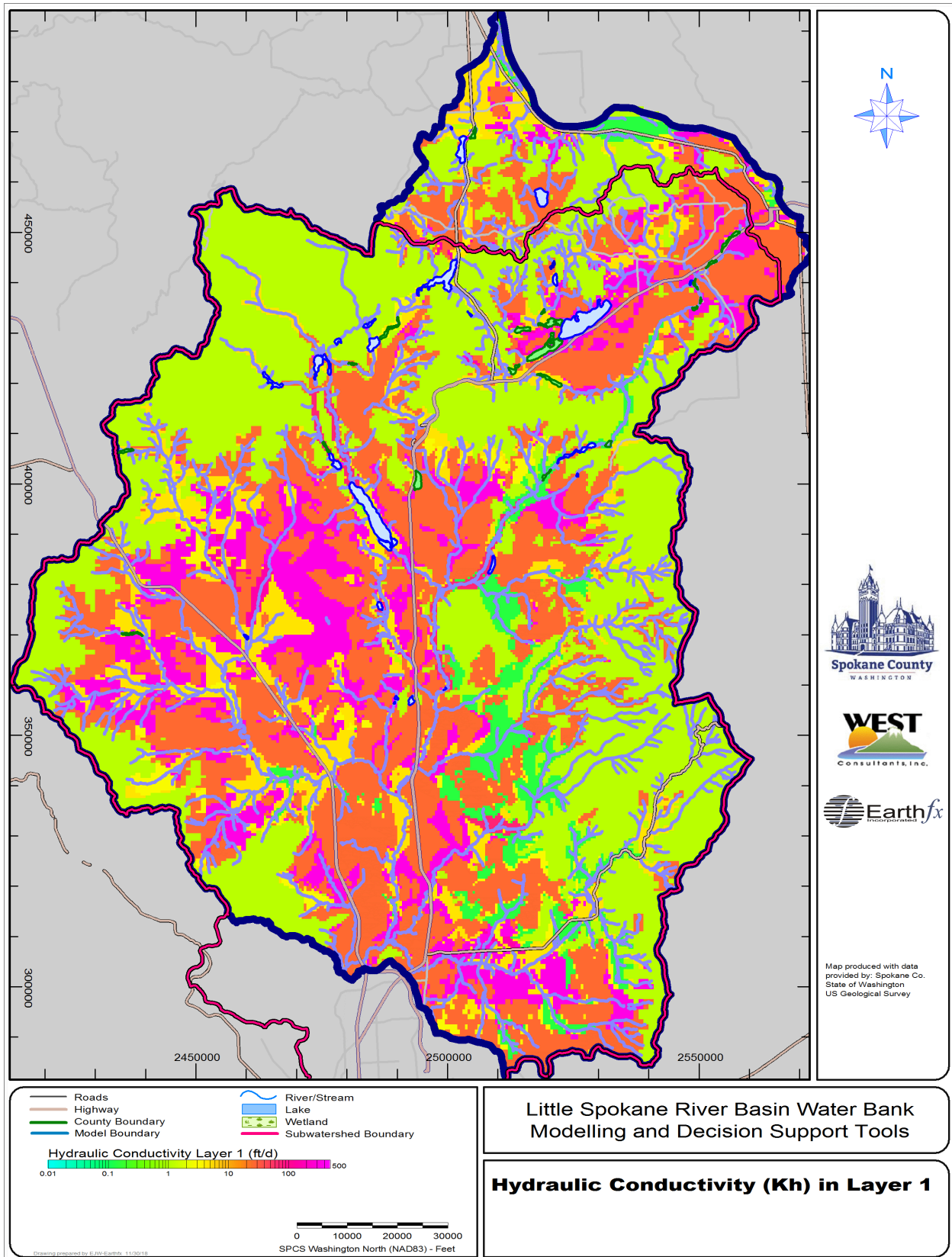


Figure 8.10: Hydraulic conductivity distribution in model layer 1.

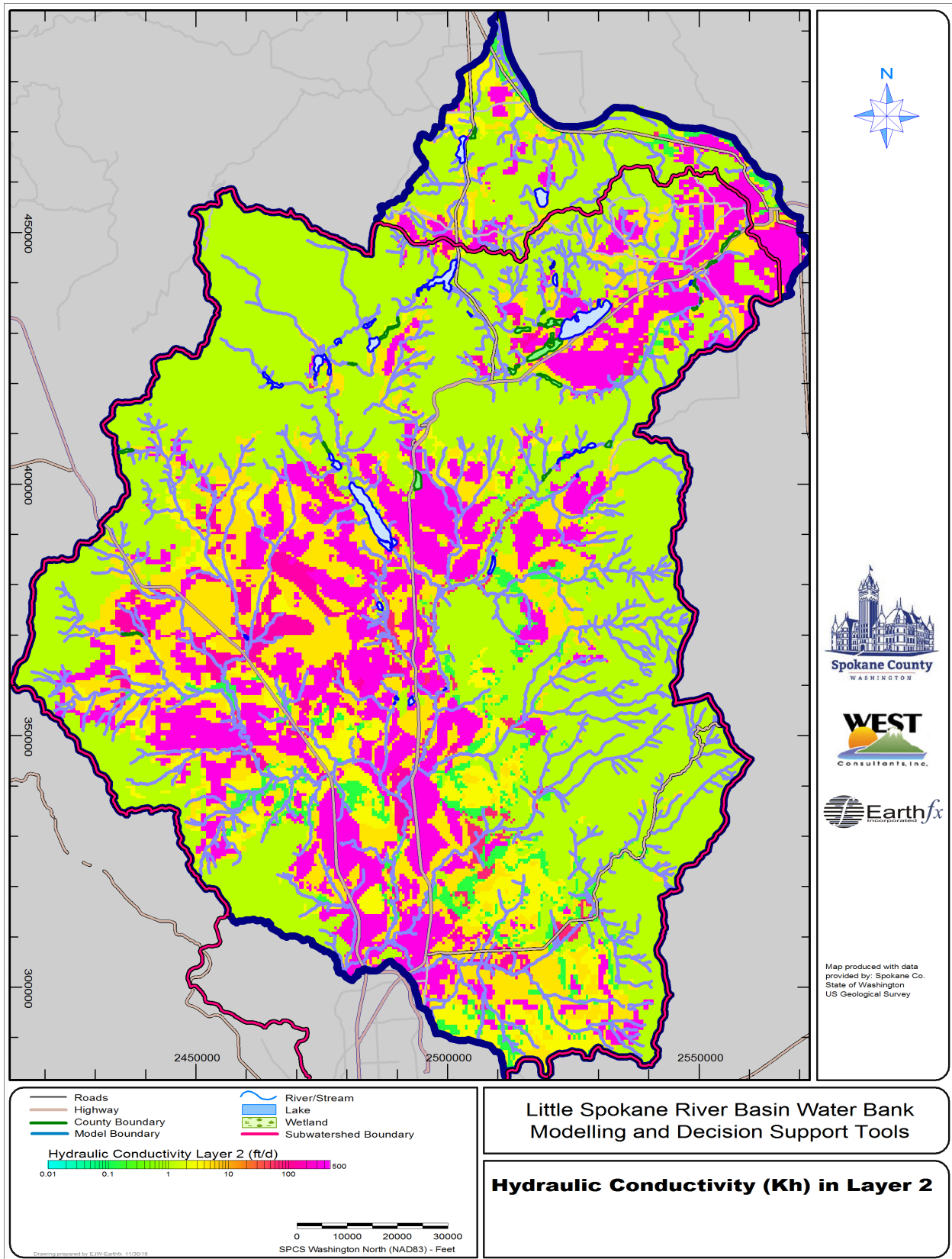


Figure 8.11: Hydraulic conductivity distribution in model layer 2.

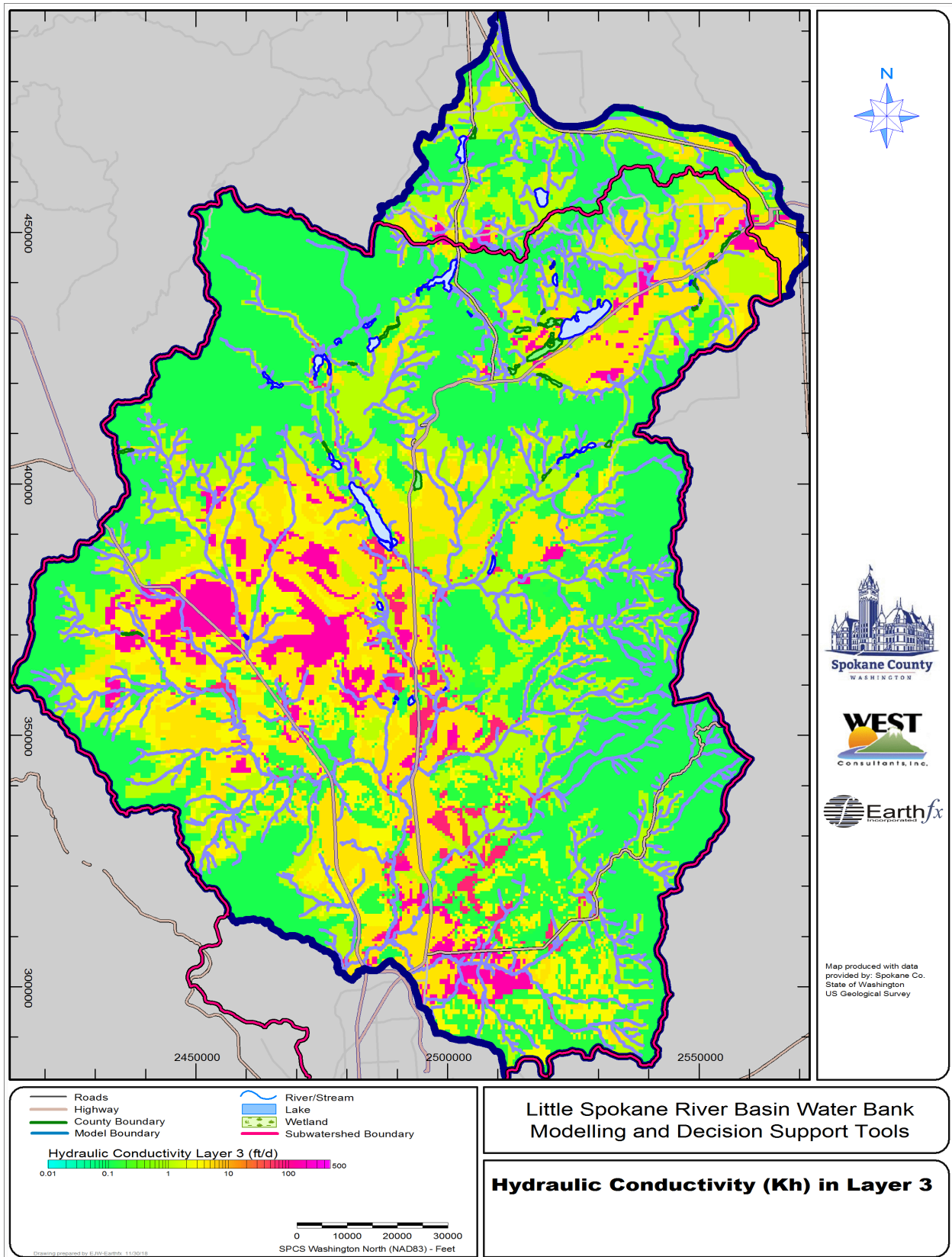


Figure 8.12: Hydraulic conductivity distribution in model layer 3.

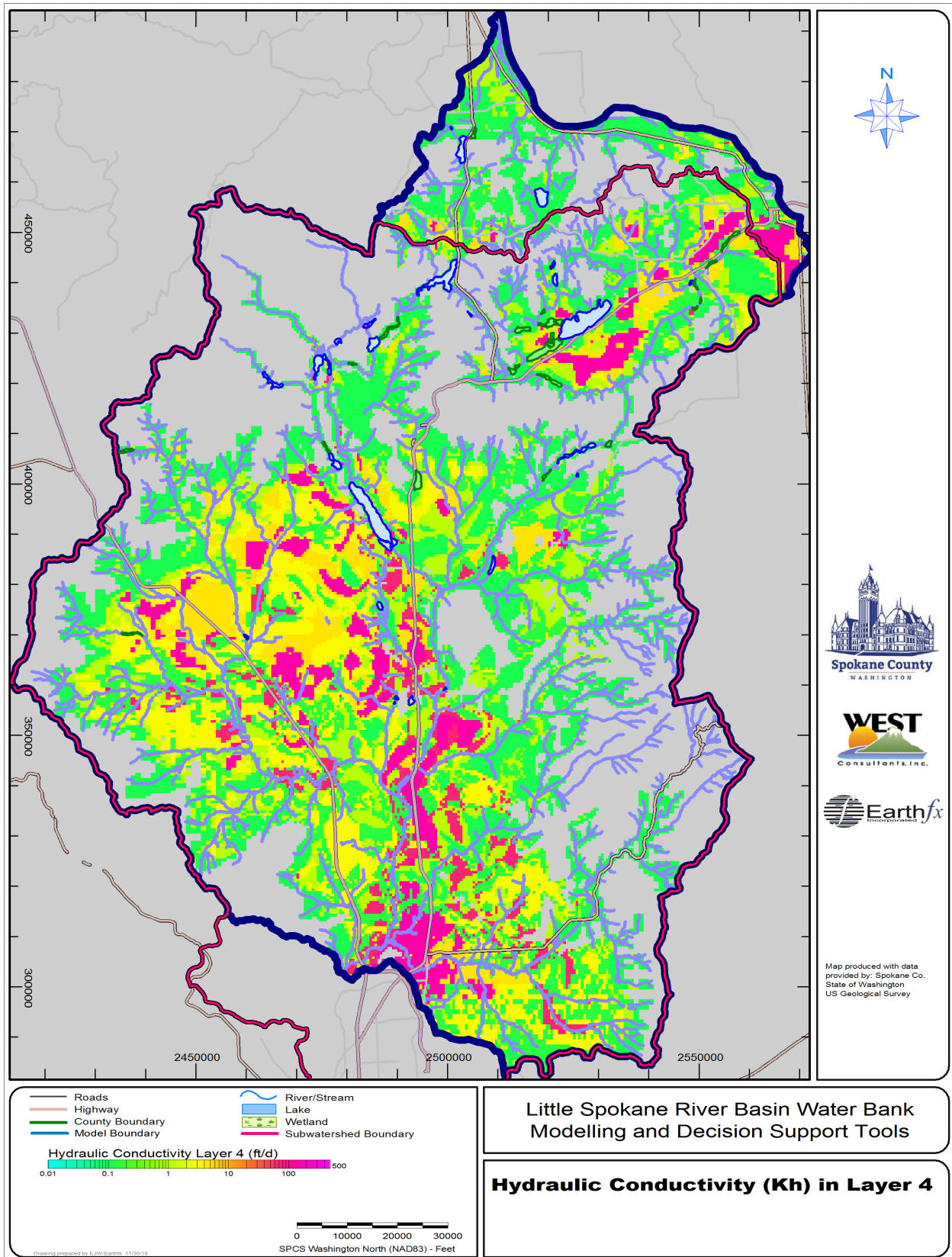


Figure 8.13: Hydraulic conductivity distribution in model layer 4 (grey areas within the model boundary represent cells beneath the unweathered bedrock unit).

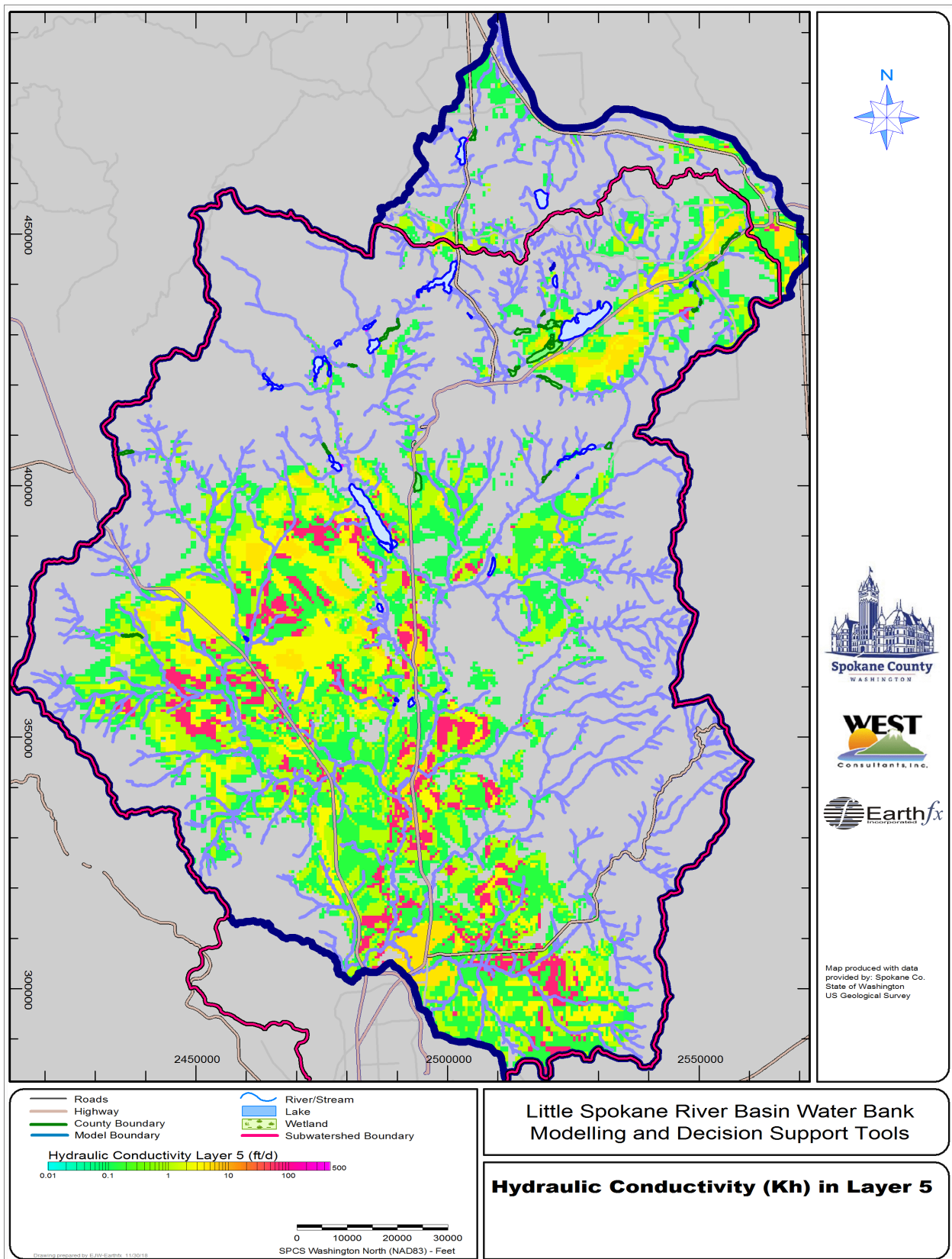


Figure 8.14: Hydraulic conductivity distribution in model layer 5.

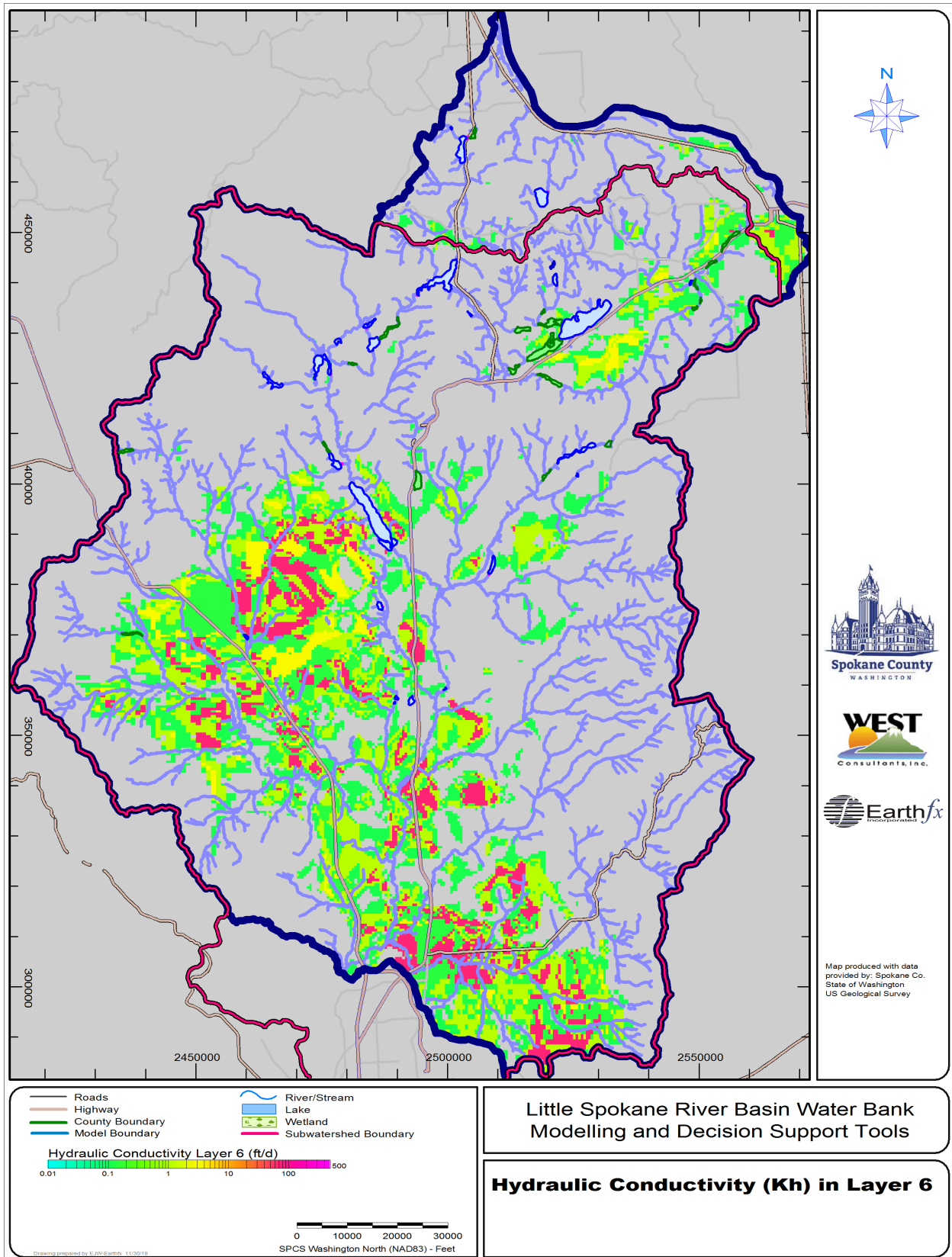


Figure 8.15: Hydraulic conductivity distribution in model layer 6.

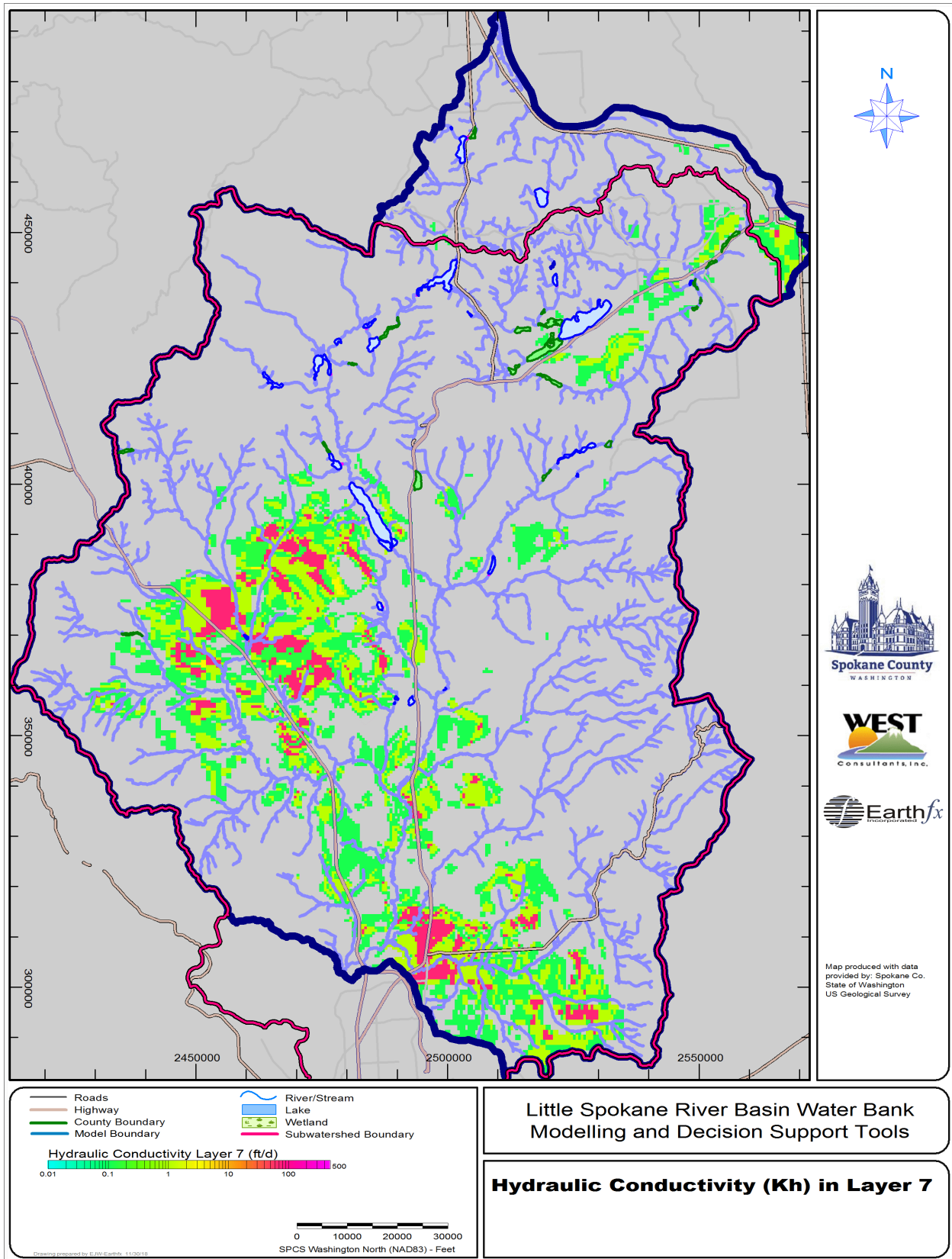


Figure 8.16: Hydraulic conductivity distribution in model layer 7.

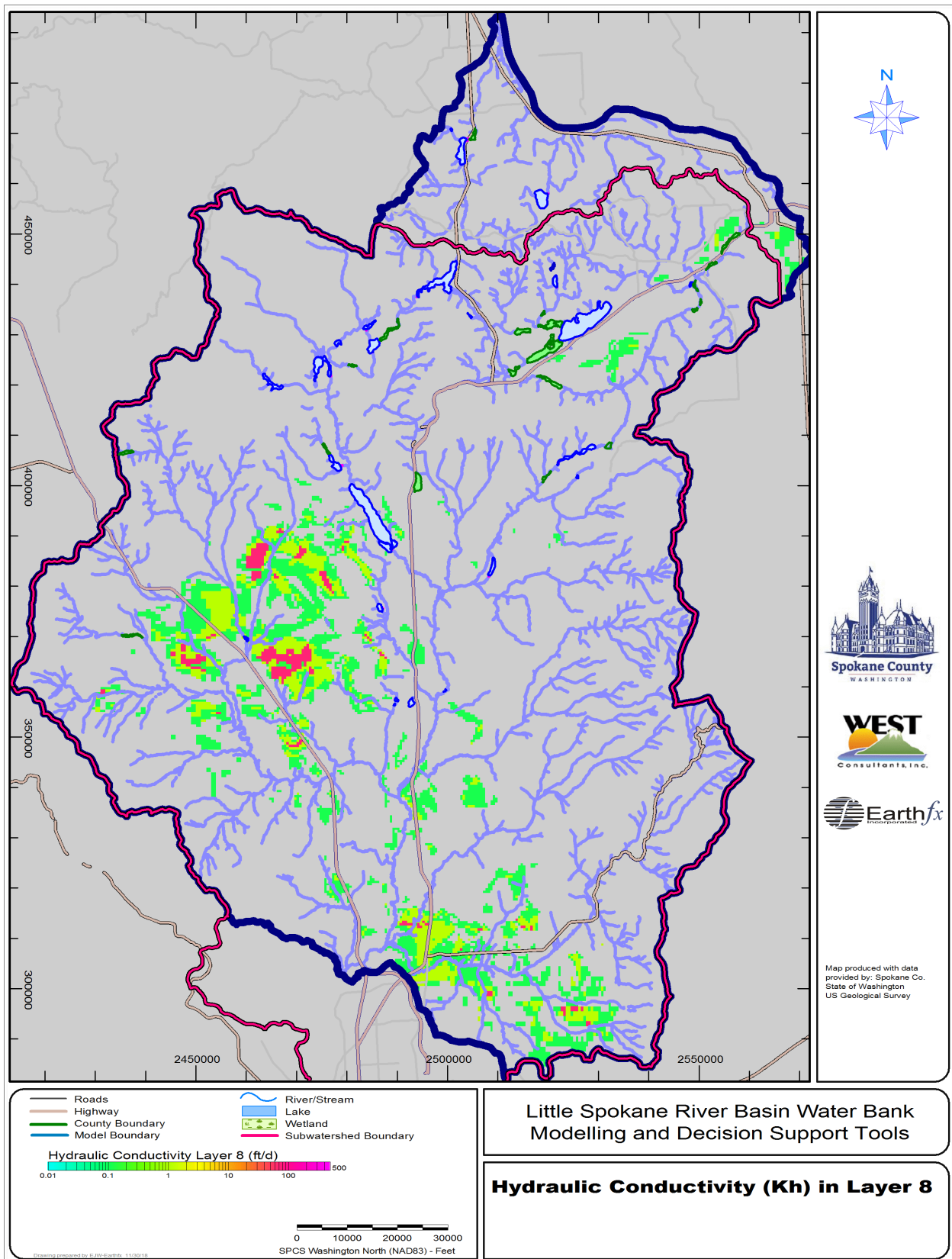


Figure 8.17: Hydraulic conductivity distribution in model layer 8.

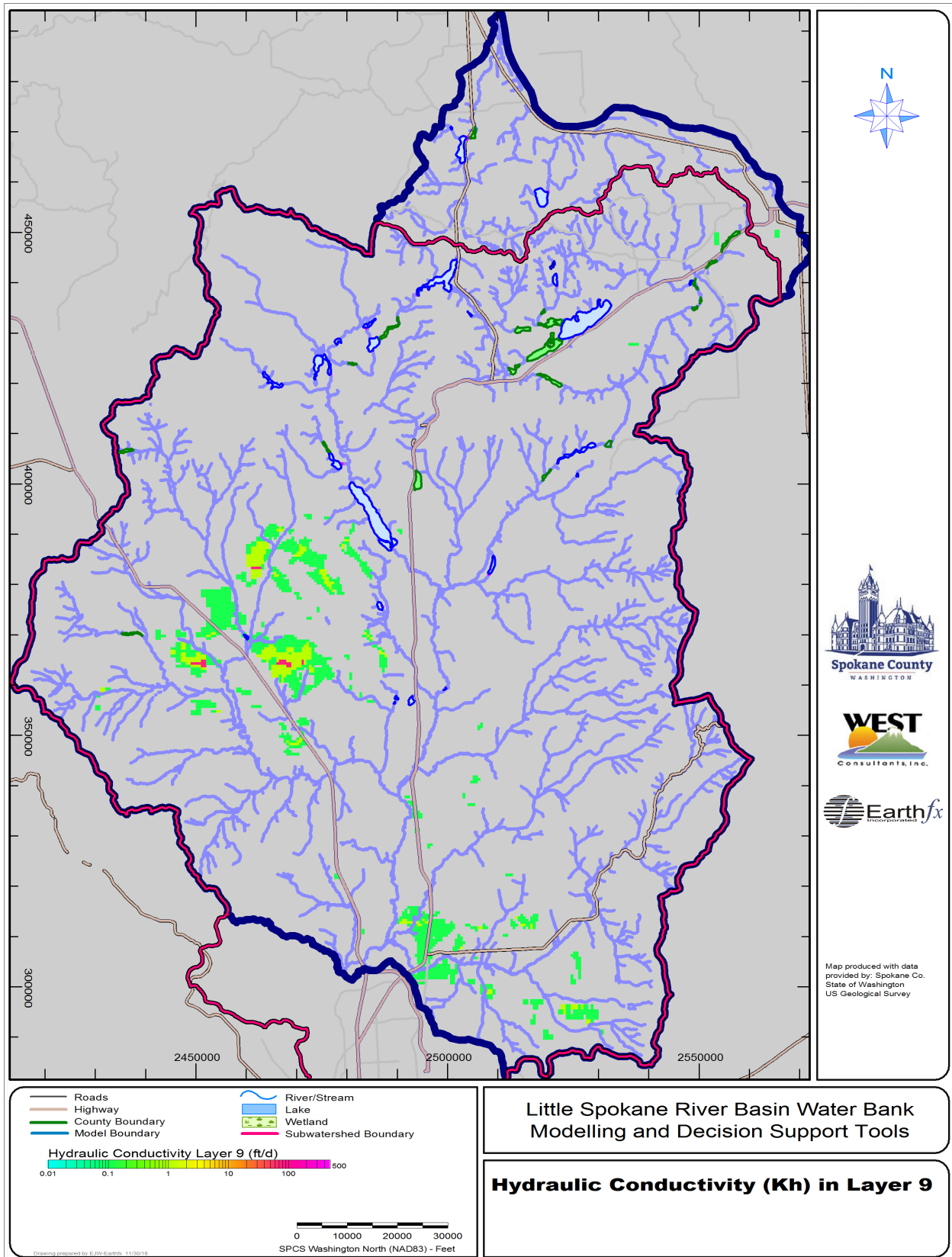


Figure 8.18: Hydraulic conductivity distribution in model layer 9.

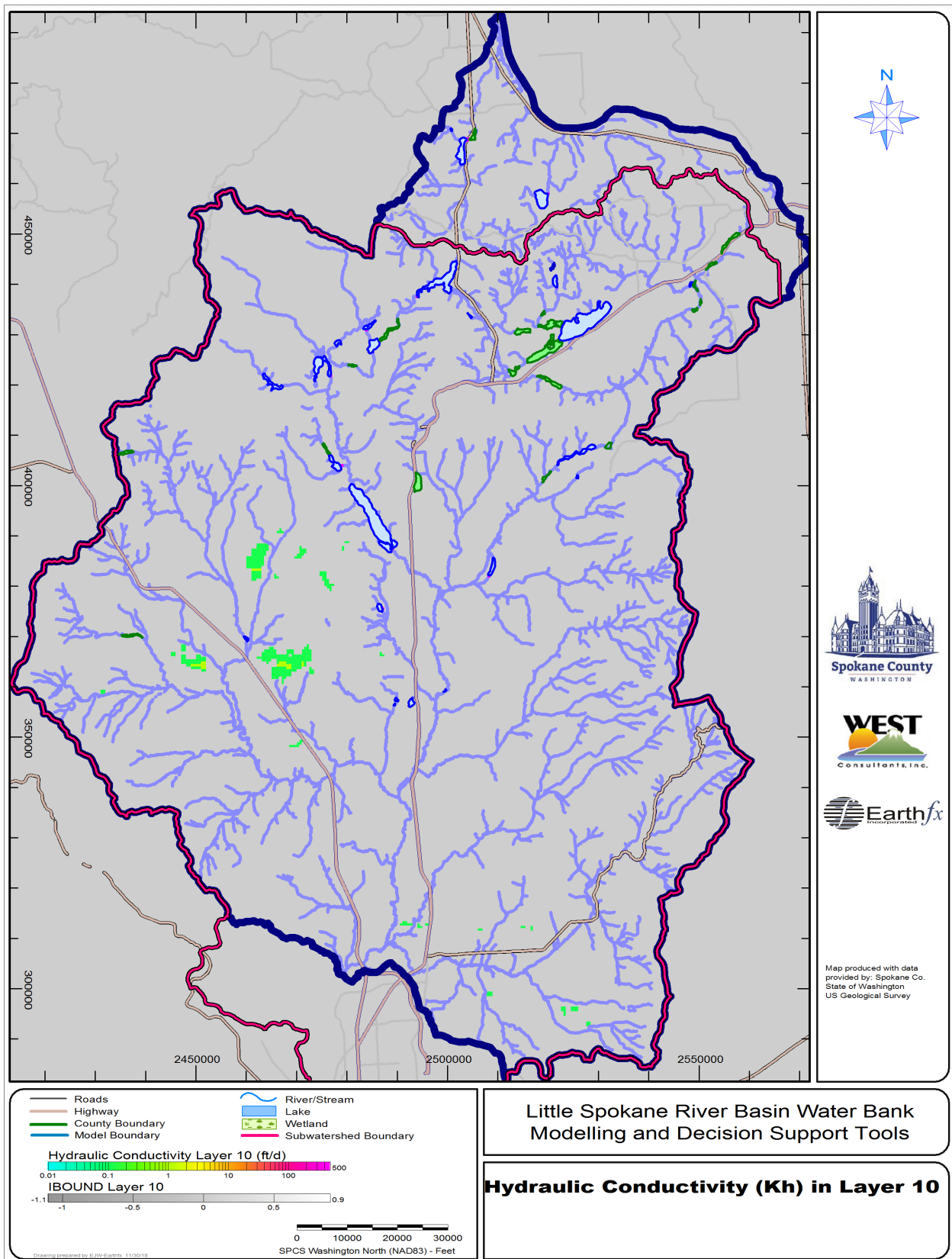


Figure 8.19: Hydraulic conductivity distribution in model layer 10.